Scintillator-based ion beam profiler for diagnosing laser-accelerated ion beams

J. S. Green*[a], M. Borghesi[b], C. M. Brenner[a,c], D. C. Carroll[c], N. P. Dover[d], P. S. Foster[a,b], P. Gallegos[a,c], S. Green[f], D. Kirby[e], K.J. Kirkby[g], P. McKenna[c], M. J. Merchant[g], Z. Najmudin[d], C. A. J. Palmer[d], D. Parker[e], R. Prasad[b], K.E. Quinn[b], P. P. Rajeev[a], M. P. Read[a], L. Romagnani[b], J. Schreiber[d], M. J. V. Streeter[d] O. Tresca[c], M. Zepf[b] and D. Neely[a,c]

[a]Central Laser Facility, STFC, Rutherford Appleton Laboratory, Chilton, Didcot, OX11 0QX, UK
[b]Department of Physics and Astronomy, Queens University, Belfast, BT7 1NN, UK
[c]SUPA, Department of Physics, University of Strathclyde. Glasgow, G4 0NG, UK
[d]Blackett Laboratory, Imperial College London, SW7 2BZ, UK
[e]School of Physics and Astronomy, University of Birmingham, Birmingham, B15 2TT, UK
[f]Department of Medical Physics, University Hospital Birmingham, Birmingham, B15 2TH, UK
[g]Department of Physics, University of Surrey, Guildford, GU2 7XH, UK

*James.Green@stfc.ac.uk; phone 44 1235-445963; fax 44 1235-445888;

ABSTRACT

Next generation intense, short-pulse laser facilities require new high repetition rate diagnostics for the detection of ionizing radiation. We have designed a new scintillator-based ion beam profiler capable of measuring the ion beam transverse profile for a number of discrete energy ranges. The optical response and emission characteristics of four common plastic scintillators has been investigated for a range of proton energies and fluxes. The scintillator light output (for 1 MeV > E_p < 28 MeV) was found to have a non-linear scaling with proton energy but a linear response to incident flux. Initial measurements with a prototype diagnostic have been successful, although further calibration work is required to characterize the total system response and limitations under the high flux, short pulse duration conditions of a typical high intensity laser-plasma interaction.

Keywords: Laser, plasma, proton, ion, acceleration, scintillator

1. INTRODUCTION

Ultra-intense (> 10^{19} Wcm^{-2}), short-pulse laser-plasma interactions typically produce a broad range of ionizing radiation with characteristic pulse durations on the order of picoseconds. These unique pulsed sources of high energy electrons, X-rays, neutrons and ions have numerous potential applications. Laser-accelerated ions in particular are of great interest, with applications envisioned in cutting-edge technologies such as radiotherapy[1], inertial confinement fusion (ICF)[2] and accelerator injectors[3]. The high brightness, short pulse duration and high degree of laminarity make laser-accelerated ion beams an attractive future alternative to conventional accelerator sources. The prospect of a compact, tunable laser-driven ion source has motivated experimental and theoretical interest world-wide and with this a requirement for new, advanced ion diagnostics.

In recent years an increasing number of high repetition rate, ultra-intense laser facilities have been commissioned, capable of delivering high power laser pulses on to target at unprecedented rates. The Astra Gemini laser facility[4], based at the Central Laser Facility, can deliver two 0.5 PW beams at a rate of one shot per minute, permitting thorough investigations into the optimization of laser-acceleration parameters. High shot rates necessitate high repetition-rate diagnostics, capable of acquiring data at 1 Hz or faster in the near future, whilst maintaining the spatial and spectral resolution offered by conventional, passive diagnostics that are useable at only very low shot rates. The placing of diagnostics in a high vacuum environment also drives the requirement for in-situ diagnostics that are remote operable by the user.

Current laser-accelerated ion diagnostics typically characterize the ion beam spectral profile, flux and spatial distribution. In order to diagnose the range of ion energies present in the beam a Thomson parabola spectrometer[5] is often used. The Thomson parabola spectrometer consists of parallel electric and magnetic fields which disperse a narrow sample of the incoming beam as a function of particle energy and charge to mass ratio. Analysis of the parabolas formed at the detection plane reveals the beam's species and spectral content. Columbia Resin 39 (CR-39) nuclear track detector[6] is typically used as a detector, yielding absolute ion numbers but requires labor intensive developing and scanning. Each individual ion detected forms a 'pit' (when etched in NaOH) on the CR-39, hence the dose dynamic range is limited by individual ion pits overlapping at high fluxes.

In order to diagnose the ion beam spatial profile a 'stack detector' is usually employed. The stack detector consists of multiple layers of Radiochromic film[7] and/or CR-39 that are sandwiched together and placed in the beam path, typically ~50 mm from the laser-irradiated target. The stack will have a thin, opaque filter on the front to prevent debris damage and direct exposure to the laser pulse. Since ions experience the greatest rate of energy loss, dE/dx, just before they are stopped (the Bragg peak), it can be deduced that the lowest energy (and heaviest) ions will be stopped at the front layers of the stack, while the higher energies propagate through the stack, depositing most of their energy in the deeper layers (see Figure 1). By calculating the Bragg curves for a particular stack composition it is possible to associate a narrow range of stopped beam energies for each layer. Hence a spectrally resolved 2D beam profile of the ion beam can be constructed over a range of ion energies and a total dose calculated.

The spatial resolution of RCF is typically of the order of 0.25 μm with a dose dynamic range of ~ 10^4 depending on the specific type of film used. The resolution of the ion spectrum that can be deconvolved from the stack is dependent on the thickness of each layer. While an invaluable tool for diagnosing laser-accelerated ion beams on single shot facilities, RCF and/or CR-39 stacks are too costly, as well as time and labor intensive, for use on the latest high repetition-rate laser systems.

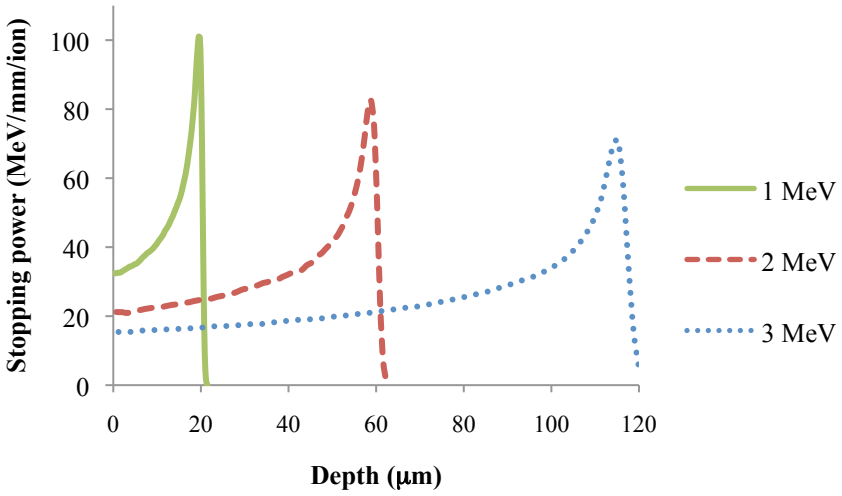

Figure 1. Stopping power of protons inside a stack of RCF. The lowest energy protons are stopped close to the front surface, while the higher energies propagate further into the stack. The majority of the dose in each sheet of RCF is mostly made up of a narrow range of proton energies whose Bragg peaks fall within the width of the film.

Recent work has focused on developing and characterizing active ion detectors for use in new, and existing, diagnostics. We should add that by 'active' we mean that the detector does not require development or scanning to be read out. Micro-channel plates (MCPs) have been used as a replacement for CR-39 as a Thomson parabola detector, converting the ion signal into an optical signal that can be read using a charge-coupled device (CCD). However care has to be taken when using MCPs too close to the laser-plasma interaction as they can be easily damaged. They are also unsuitable for measuring the spatial and spectral profile of the beam as they are unable to differentiate ion energies without first dispersing the beam.

Organic scintillators have been used in the accelerator and medical communities for years and we have recently explored their use as detectors of short pulse ion beams. Such scintillators can convert any form of ionizing radiation into light through a fluorescence process based on multiple molecular transitions. Anthracene is a common organic scintillator which can be dissolved into a liquid solvent or solid polymer material. As the scintillator absorbs energy from the incoming ionizing radiation, electrons are promoted to excited states before quickly transitioning to the ground state leading to prompt fluorescence. The fluorescence decays exponentially with a characteristic decay time of ~ns.

Initial tests of plastic (polyvinyltolouene based) scintillators as an imaging medium for Thomson parabola spectrometers were successful[8] leading us to develop a new in-situ diagnostic capable of imaging a laser-accelerated ion beam over a number of discrete energy ranges. In order for plastic scintillators to be viable in a range of ion diagnostics it is crucial that these detectors are calibrated over a range of incident ion energies and fluxes. This enables them to provide quantitative data on the absolute ion yield and hence estimate the laser-ion conversion efficiency.

2. THE ION BEAM SPATIAL PROFILER

The ion beam spatial profiler replicates the working principal of the RCF / CR-39 stack, using organic scintillators as an active imaging medium. By placing multiple scintillators together and exposing them to the ion beam, each scintillator will respond to a different ion energy range. By imaging the light emitted from each scintillator a 2D 'footprint' of the ion beam can be collected for multiple beam energies.

In the latest revision of the diagnostic the scintillator stack is housed in a light-shielded box which can be placed close to the laser-plasma interaction. A camera lens is used to image the scintillator stack over a distance of 5-20 cm (depending on the size of the ion beam to be imaged), and the light is coupled from the diagnostic head into an intensified CCD camera via a high resolution (800 x 800 pixels) Schott fiber optic bundle (see Figure 2). The use of a fiber optic bundle simplifies the diagnostic alignment process and reduces the risk of electromagnetic pulse (EMP) and X-ray damage to the CCD camera.

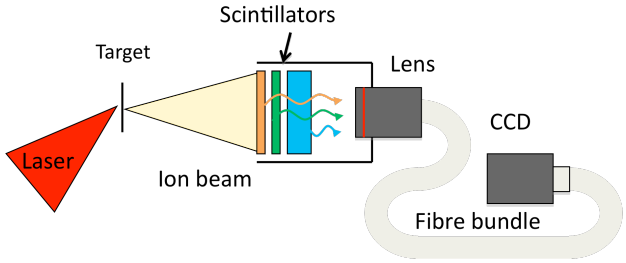

Figure 2. Schematic of the ion beam spatial profile monitor. Higher energy protons are stopped in the shorter wavelength scintillators further in the stack. The combined optical signal is collected and relayed to a CCD camera via a fiber optic bundle.

In order to distinguish between the optical signals emitted by each scintillator we have investigated the use of multiple scintillators, each with a different emission spectrum. So far we have tested four anthracene-based scintillators; BC-408 and BC-422Q manufactured by Saint-Gobain Crystals and EJ-260 and EJ-264 manufactured by Eljen Technology. The typical emission spectra for each scintillator have been measured and are shown in Figure 3.

Since the scintillators are sensitive to all forms of ionizing radiation care must be taken when analyzing the data. Initial tests indicate that when using thin (sub mm) scintillators to observe heavy ions or lower energy protons (< 10 MeV) the dominant signal will be due to that of the ions owing to their steep Bragg peak stopping profile. However when lower proton fluxes are predicted, or thick scintillators are used, then a non-negligible level of fluorescence due to high energy electrons or X-rays will be produced. To counter this, gated CCD cameras can be used to gate out the initial flash due to electrons and X-rays, provided that both the CCD camera and scintillator have a sufficiently short response time.

2.1 Scintillator emission spectra

Figure 3 shows that the emission spectra of the scintillators cover a range of wavelengths from 325 nm to 750 nm, with some overlap inbetween. Both the EJ-260 and EJ-264 have blue tails in their spectra which can be attributed to the wavelength shifting process in these longer wavelength scintillators. Each scintillator contains additional doping which absorbs the initial (blue) scintillated light and re-emits it at longer wavelengths. For thin (sub mm) sheets this process is not 100% efficient, however for thicker samples this short wavelength tail can be eliminated. For this reason the longer wavelength scintillators need to be placed at the front of the stack (as in Figure 1) in order to prevent absorption of shorter wavelength scintillated light from other layers.

To resolve the ion beam profile at each energy range, the optical signal from each scintillator must be clearly separable in order that they can be split and imaged individually at the CCD camera. In order to achieve this a thin, polymer colored filter is placed between each scintillator to act as a long pass filter (see modified output in Figure 4 for a three color system). By placing the longest wavelength scintillator (EJ-264) at the front of the stack, and the shortest wavelength (BC-408 or BC-422Q) towards the rear, a narrow portion of each signal can be isolated at the detector end.

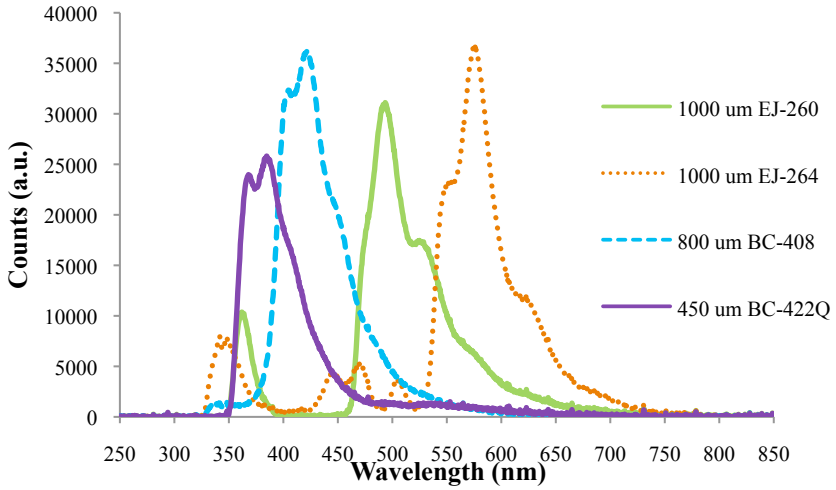

Figure 3. Optical emission spectra for BC-422Q, BC-408, EJ-260 and EJ-264 thin organic scintillators. Spectra were obtained by illuminating each scintillator with a 2.5 MeV proton beam.

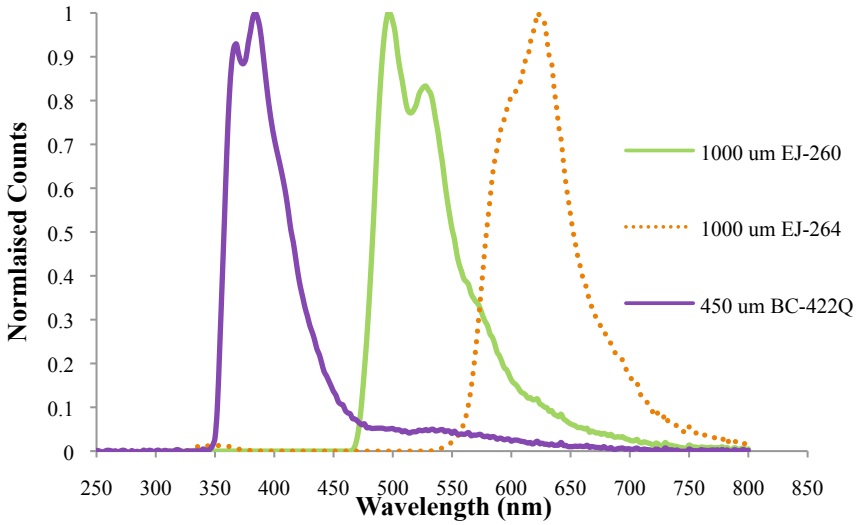

Figure 4. Predicted optical emission spectra for a combination of BC-422Q, EJ-260 and EJ-264 thin organic scintillators. Emission curves have been normalized as they do not take into account the incident ion flux on each layer.

2.2 Scintillator response as a function of proton energy

In order to characterize the response of each scintillator to a range of proton fluxes and energies, each material was tested individually using two tunable, monoenergetic proton sources. The light from each scintillator was collected using a fixed CCD lens and an Andor iXon intensified CCD camera. For the lowest energies (250 keV – 4 MeV) the tunable Tandetron accelerator at the Surrey Ion Beam Centre was used. For higher energies (3 MeV – 28 MeV) calibration tests were carried out using the University of Birmingham Cyclotron. While the typical currents (1-10 nA) produced by each facility differed, we have scaled the CCD counts accordingly, having first confirmed a linear response to (see Figure 6 (Left)) the fluxes being considered here.

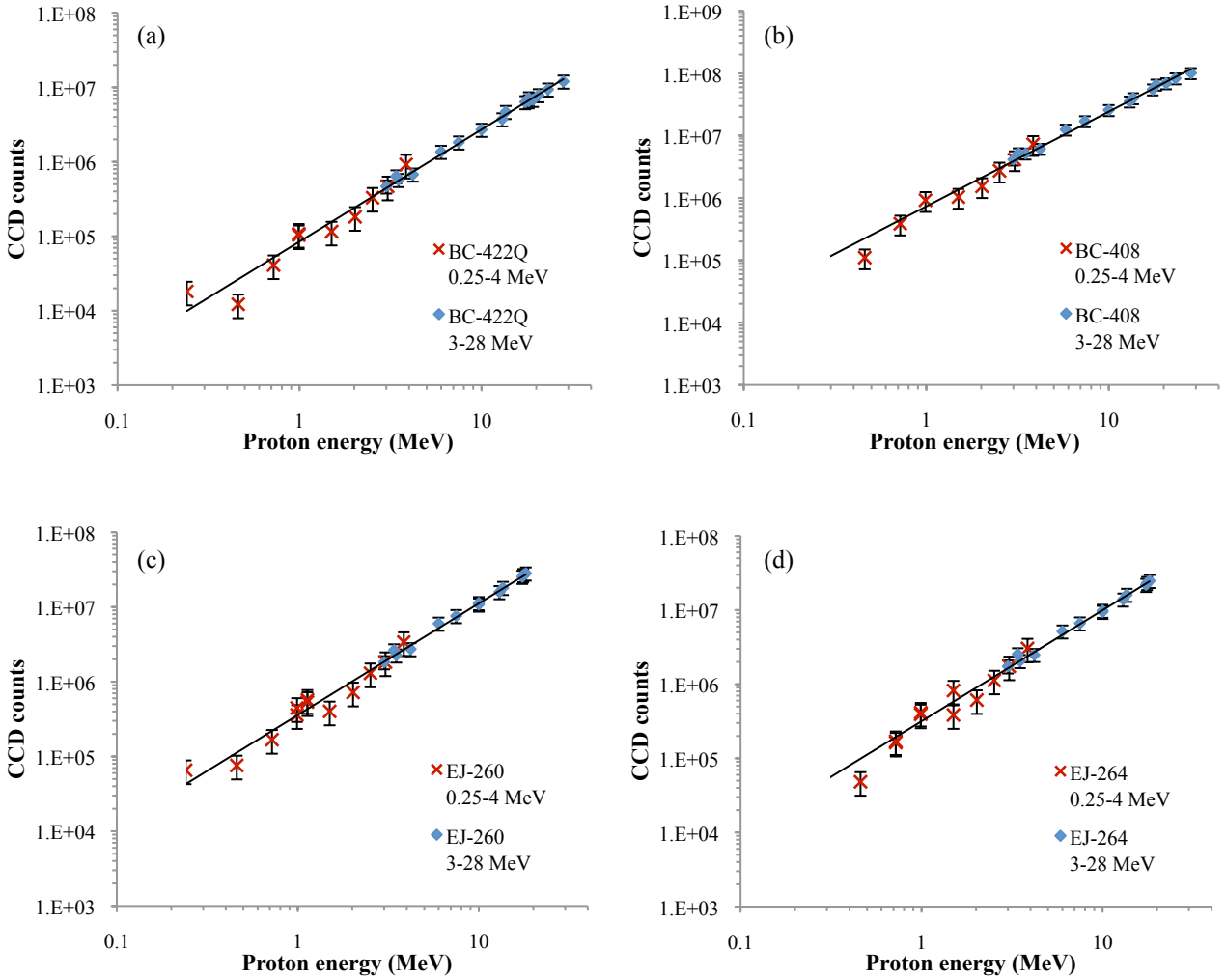

Figure 5. Proton response data for (a) BC-422Q, (b) BC-408, (c) EJ-260 and (d) EJ-264 thin organic scintillators together with empirical fits.

The response curves for each scintillator are shown in figure 5. The optical output of the BC-422Q and BC-408 scintillators was found to be proportional to proton energy to the powers of $E_p^{1.50 +/- 0.04}$ and $E_p^{1.52 +/- 0.04}$ respectively. For the Eljen Technologies EJ-260 and EJ-264 scintillators, the light output was found to scale similarly with proton energy

as $E_p^{1.49 +/- 0.04}$ and $E_p^{1.50 +/- 0.04}$ respectively. As expected these anthracene-doped scintillator response data are consistent with those obtained by Smith et al. for anthracene crystals[9].

Care must be taken when using the above scalings when calibrating experimental results for several reasons. Firstly the response of the above plastic scintillators at low energies (< 1 MeV) appears to deviate from the quoted response, tending towards a more linear response. Secondly the response of a scintillator will change depending on the length and degree of previous exposure to ionizing radiation. Continuous exposure to high fluxes of ionizing radiation will reduce a scintillator's light output dramatically[10].

In order to examine the effect of high proton fluxes on scintillator response a 3 MeV proton beam was focused down to a spot size of just 1.7 mm (FWHM), using a beam current of 10 nA. The scintillator light output was then recorded at regular intervals (see Figure 6 (Right)). The scintillator response clearly falls rapidly as the incident dose accumulates, before leveling out after several minutes. The sharp reduction in light output is most likely concentrated around the Bragg peak for the incident proton energy. The drop in scintillation could be due to damage to the polyvinyltolouene base material (reducing optical transmission) or to the scintillator compound itself (reducing optical emission).

The continuous wave nature of the proton source used here might be expected to exacerbate any damage, reducing material recovery times, however future high-repetition rate laser systems might require operation on a quasi-continuous basis. Under these conditions accurate flux measurements using organic plastic scintillators would require a careful choice of illumination area, especially in the case of monoenergetic ion beams. Further studies need be conducted to quantify the effect of continuous wave and short-pulse fluxes of protons on scintillator response and to identify the nature of both the reversible and irreversible damage.

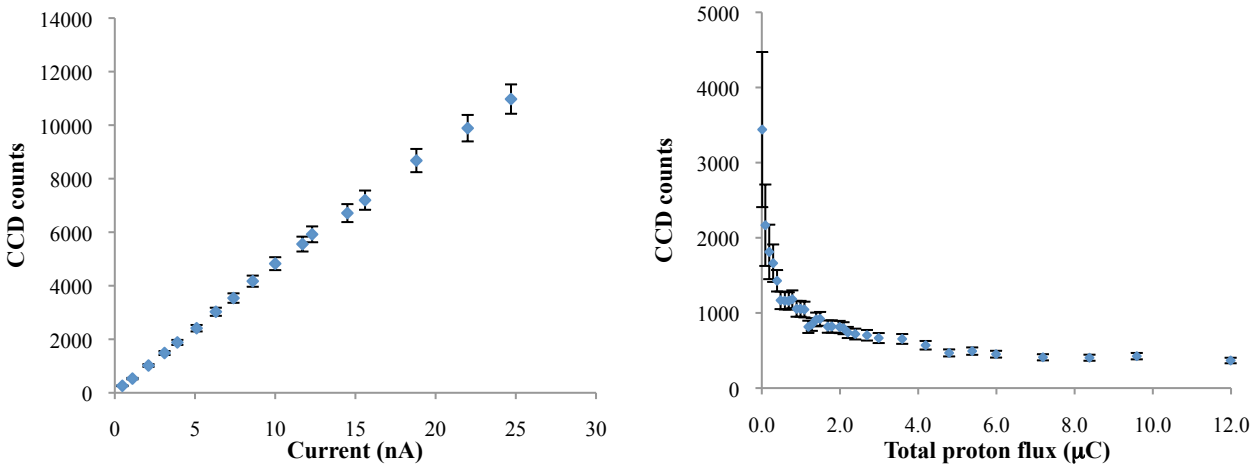

Figure 6. (Left) BC-408 scintillator response as a function of beam current. (Right) EJ-260 scintillator response as a function of total incident proton flux when irradiated with a focused current of 10 nA for 12 minutes.

3. INITIAL RESULTS

An experiment was performed on the Astra Gemini laser facility at the Rutherford Appleton Laboratory to investigate laser-driven ion acceleration under ultra-intense, short-pulse laser conditions. 10 J of laser energy was delivered onto target with a pulse duration of 50 fs using an f/2 off-axis parabola, yielding a peak focused intensity of 10^{21} Wcm^{-2}. For some shots an increased level of laser contrast (the ratio of the main pulse intensity to that of any amplified spontaneous emission) was required, so a pair of plasma mirrors[11] were used to increase the laser contrast from ~10^7 to ~10^{10}. The combined reflectivity of the plasma mirrors was found to be 48%, resulting in a peak intensity on target of ~ $5x10^{20}$ Wcm^{-2}.

Laser-accelerated protons normal to the target rear surface were diagnosed using a prototype scintillator-based beam profiler that utilized both BC-408 and BC-422Q scintillators, producing two beam profiles over energy windows of 5-8 MeV and 8-10 MeV respectively. The diagnostic was placed in the lower half of the proton beam, approximately 12 cm from the rear of the target surface. Protons with energies below 5 MeV and heavy ions were stopped by a protective, light-tight debris plate that was placed over the front of the diagnostic. A beam splitting prism with separate low and high pass filters over each half was used to resolve each channel on to a Princeton Instruments gated CCD camera.

A number of targets were irradiated, including metallic and dielectric foils, ranging in thickness from 5 nm to 20 μm. Figure 7 shows an example of the two channel proton beam imaging, showing a low emittance (< 10 degrees) proton beam from a 100 nm Al target under high contrast laser conditions. Figure 8 demonstrates the diagnostics capability to monitor beam divergence, flux and pointing on a shot-to-shot basis.

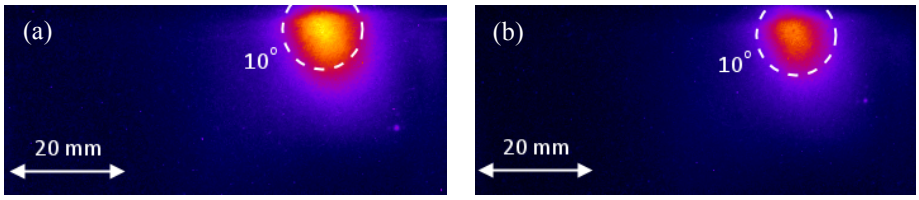

Figure 7. Proton (half) beam transverse profiles for a 100 nm Al target at (a) 5-8 MeV (b) 8-10 MeV. The 10 degree full cone angle is shown for reference.

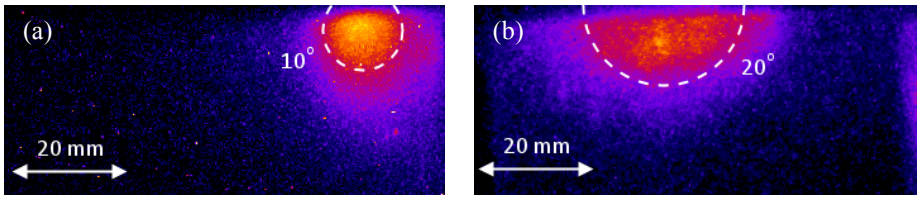

Figure 8. Proton (half) beam transverse profiles for a 6 μm Al target under (a) high contrast (b) low contrast laser conditions.

4. FUTURE WORK

Over the next few years we predict that the demand for in-situ, high repetition rate diagnostics suitable for characterizing laser-generated radiation will increase significantly. The work presented here marks the initial steps towards a fully-calibrated, multi-channel ion beam imaging system suitable for deployment on a range of laser facilities. While the initial experimental results have been positive, it is clear that care must be taken when analyzing any results if quantifiable data is to be extracted.

Cross-calibration of the scintillator-based beam profile monitor with existing passive media methods (e.g. RCF stacks) on upcoming ultra-intense laser-plasma experiments will act as a useful evaluation of the difference (if any) in scintillator response to a pulsed source as opposed to the continuous accelerator sources presented here. Such an experiment will also allow a direct comparison of the scintillator spatial resolution over a range of ion energies.

Additional work on the damage threshold and lifetime of plastic scintillators also needs to be undertaken, with the aim of characterising the usable dynamic range for consistent operation under the extreme conditions of a laser-plasma interaction. Indentifying the mechanisms of radiation-sourced scintillator damage will enable us to identify new preventative measures or chemical compounds that could be used to minimize any fluctuations in diagnostic operation during use.

5. ACKNOWLEDGMENTS

The authors gratefully acknowledge the assistance of the Central Laser Facility staff at the Rutherford Appleton laboratory. We would also like to acknowledge the valuable facility access and useful discussions provided by the Surrey Ion Beam Centre and University of Birmingham. The work has been supported as part of the LIBRA EPSRC grant EP/E035728/1.

6. REFERENCES

[1] Bulanov S. V. and Khoroshkov V. S. "Feasibility of using laser ion accelerators in proton therapy," Plas. Phys. Rep. 28(5), 453-456 (2002).
[2] Roth M. et al., "Fast Ignition by Intense Laser-Accelerated Proton Beams," Phys. Rev. Lett. 86(3), 436-439 (2001).
[3] Krushelnick K. et al., "Energetic proton production from relativistic laser interaction with high density plasmas," Phys. Plas. 7(5), 2055-2061 (2000).
[4] Hooker C. J., "The Astra Gemini project - A dual-beam petawatt Ti:Sapphire laser system," J. Phys. IV France 133, 673-677 (2005).
[5] Sakabe S. et al. "Modified thomson parabola ion spectrometer of wide dynamic range," Rev. Sci. Inst. 51, 1314 (1980).
[6] Fleischer R. L., Price P. B and Walker R. M., "Ion Explosion Spike Mechanism for Formation of Charged-Particle Tracks in Solids," J. Appl. Phys. 36(11), 3645-3652 (1965).
[7] Klassen N. V. et al. "GafChromic MD-55: Investigated as a precision dosimeter," Med. Phys. 24, 1924 (1997).
[8] Green J. S. et al. " Enhanced proton flux in the MeV range by defocused laser irradiation," New J. Phys. 12, 085012 (2010).
[9] Smith D. L. et al. "Measurement of the response of several organic scintillators to electrons, protons and deuterons," Nucl. Inst. Meth. 64(2), 157 (1968).
[10] Hamada M. M. et al., " Radiation damage studies on the optical and mechanical properties of plastic scintillators," Nucl. Inst. Meth. A 422, 148 (1999).
[11] Ziener Ch et al., "Specular reflectivity of plasma mirrors as a function of intensity, pulse duration, and angle of incidence," J. Appl. Phys. 93, 768 (2003).